Pure & Appl. Chem., Vol. 64, No. 6, pp. 815–823, 1992.
Printed in Great Britain.

Quantification of 1-D and 2-D magnetic resonance time domain signals

R. de Beer, D. van Ormondt, and W.W.F. Pijnappel

Applied Physics Laboratory, Delft University of Technology, P.O. Box 5046, 2600 GA, Delft The Netherlands, E-mail: ormo@dutnsi2.tudelft.nl

Abstract - This paper addresses quantification of uniformly sampled time domain signals by means of State Space modelling (based on Singular Value Decomposition (SVD) and Vandermonde Decomposition). An advantage of State Space modelling is that a specific model function and starting values of model parameters need not be provided by the user. A disadvantage is that if a detailed model function and prior knowledge about model parameters is available, such information cannot be accommodated. Aspects considered are, among other things, 1) Reduction of the computation time of SVD by invoking the Lanczos algorithm and exploiting the Hankel symmetry of the data matrix, 2) Handling of nonexponentially damped signals, 3) Rank-related problems with 2-D signals and their solution.

INTRODUCTION

The subject of this paper is quantification of time domain signals. By quantification we mean introduction of a model function that describes the signal at hand, and subsequent estimation of the model parameters by some numerical procedure. The strategy is to carry out the quantification directly in the domain where the measurement took place, so as to avoid having to cope with possible transformation artefacts. See e.g. (refs. *1-6*).

If a detailed model function is known, then the quantification method of choice is to fit this model function to the data by means of some nonlinear optimization procedure (refs. *7-11*), exploiting whatever prior knowledge is available. As a rule such procedures yield the best possible result. However, much expertise of the user is often required, which may constitute an unsurmountable hurdle. Furthermore, if no model function is available, use of the above mentioned optimization methods is not feasible anyway. These considerations indicate that there is also a need for simpler, suboptimal methods that do not require much user involvement and can yet bring about quantification of nondescript spectral features. Examples of such methods are Linear Prediction (ref. *12*) and State Space modelling (refs. *13,14*). These methods intrinsically wield exponentially damped sinusoids as basis functions. However, they are capable of quantifying *non*exponentially damped sinusoids by expanding such functions in terms of exponentially damped sinusoids. In this work we consider only State Space modelling which is simpler than Linear Prediction in that polynomial rooting and root selection are avoided.
This paper is organized as follows. First, we briefly review the basics of State Space modelling in terms of simple matrix algebra, using Vandermonde decomposition and Singular Value Decomposition (SVD). The way in which nonexponentially decaying signals are handled with little user involvement is indicated. Next, we show that the computation of SVD can be accelerated considerably by invoking the Lanczos algorithm combined with imposing the Hankel symmetry of the data matrix (in the 1-D case). Finally, we show that the data matrix attendant to 2-D signals poses rank problems. A solution of these problems is presented. Several applications are interspersed in the text.

STATE SPACE THEORY AND APPLICATIONS

First note that other names exist in the literature to denote State Space modelling. Of these we mention HSVD, H standing for Hankel (refs. *15-17*), Toeplitz Approximation Method (TAM, ref. *18*), and State-Variable Balancing (ref. *19*). Our treatment uses only concepts from the realm of matrix algebra (ref. *20*), avoiding the general State Space formalism (ref. *14*). When quantifying 1-D measurements, the data must first be rearranged ('inflated') from a single row into a full-blown matrix. Because of the redundancy present in such a matrix, the storage requirements and computational complexity can be limited. When quantifying 2-D measurements, the data already form a matrix in natural fashion, each data point entering only once. However, traditionally one treats the rows and columns of the latter matrix separately, as though dealing with a series of independent 1-D measurements. Our approach involves all 2-D data concurrently, in an attempt to increase the statistical performance. In order to do this for general cases, we first have to solve a problem related to the rank of a 2-D magnetic resonance data matrix. The *rank of a matrix* is the number of linearly independent rows (or columns).

1-D signals

The basic function used in the State Space formalism to model the measurement is the exponentially damped sinusoid, $f(t) = \exp[(\alpha + i\omega)t + i\varphi]$. In this function α is the damping factor ($\alpha < 0$), ω the angular frequency ($\omega = 2\pi\nu$), φ the phase, and $i = \sqrt{(-1)}$. A real-world signal, $x_n, n = 0, \ldots, N-1$, comprising a number of spectral components is modelled accordingly as a sum of K different sinusoids, i.e.

$$\hat{x}_n = \sum_{k=1}^{K} c_k f_k(t_n) = \sum_{k=1}^{K} c_k \exp(i\varphi_k) \exp[(\alpha_k + i\omega_k)t_n] \tag{1}$$

where the c_k are the amplitudes of the sinusoids $f_k(t_n)$, $k = 1, \ldots, K$, and $t_n = t_0 + n\Delta t$, $n = 0, 1, \ldots, N-1$ are the sampling times. The caret on $\hat{x}_n$ enables one to distinguish between measurement and model function. As for K, the number of exponentially damped sinusoids to be fitted, we point at the following. If the spectral components contained in the signal are all exponentially damped, in conformity with Eq.(1), then K equals of course the number of distinguishable components. However, should other forms of damping such as e.g. $\exp(\beta t^2)$ with $\beta < 0$ occur, the State Space method automatically expands each such spectral component into a sum of exponentially damped sinusoids, thus still achieving adequate parametrization (ref. *21*). See Fig. 1. Most often the user does not become involved in this aspect during execution time of the fit. It is only at the stage of *interpreting* the fitted model parameters that expert insight may be required. See (refs. *22,23*).

We shall now review the various steps leading to quantification. The starting point of the procedure is to form $L \times M$ matrices X and $\hat{X}$ from respectively the data x_n, $n = 0, \ldots, N-1$, and the model function $\hat{x}_n$, $n = 0, \ldots, N-1$, according to

$$X \stackrel{\text{def}}{=} \begin{pmatrix} x_0 & x_1 & x_2 & \cdots & x_{M-1} \\ x_1 & x_2 & \cdot & \cdot & \cdot \\ x_2 & \cdot & \cdot & & \cdot \\ \cdot & \cdot & & & \cdot \\ \cdot & \cdot & & & \\ \cdot & \cdot & & & \\ x_{L-1} & \cdot & \cdot & \cdot & x_{N-1} \end{pmatrix}, \qquad \hat{X} \stackrel{\text{def}}{=} \begin{pmatrix} \hat{x}_0 & \hat{x}_1 & \hat{x}_2 & \cdots & \hat{x}_{M-1} \\ \hat{x}_1 & \hat{x}_2 & \cdot & \cdot & \cdot \\ \hat{x}_2 & \cdot & \cdot & & \cdot \\ \cdot & \cdot & & & \cdot \\ \cdot & \cdot & & & \\ \cdot & \cdot & & & \\ \hat{x}_{L-1} & \cdot & \cdot & \cdot & \hat{x}_{N-1} \end{pmatrix}, \tag{2}$$

where all elements on an antidiagonal are equal. A matrix possessing such symmetry is called a Hankel matrix. The shape of X and $\hat{X}$ is chosen such that both L and M are greater than the number of sinusoids K in the model function, subject to the constraint $L + M = N + 1$. Often one takes $L \approx M \approx N/2$, especially when the K is known to be large. By virtue of the following property of the exponentially

damped sinusoid, namely

$$f_k(t_n) = z_k^n f_k(t_0), \quad n = 0, \ldots, N-1 \quad , \tag{3}$$

with $z_k \stackrel{\text{def}}{=} \exp[(\alpha_k + i\omega_k)\Delta t]$, $\hat{X}$ can be decomposed as

$$\hat{X} = \begin{pmatrix} 1 & \cdots & 1 \\ z_1^1 & \cdots & z_K^1 \\ \vdots & & \vdots \\ z_1^{L-1} & \cdots & z_K^{L-1} \end{pmatrix} \begin{pmatrix} c_1'' & & 0 \\ & \ddots & \\ 0 & & c_K'' \end{pmatrix} \begin{pmatrix} 1 & z_1^1 & \cdots & z_1^{M-1} \\ \vdots & \vdots & & \vdots \\ 1 & z_K^1 & \cdots & z_K^{M-1} \end{pmatrix} , \tag{4}$$

$$= \qquad \zeta_{LK} \qquad\qquad C \qquad\qquad \tilde{\zeta}_{MK} \tag{4'}$$

in which ζ_{LK} and ζ_{MK} are respectively $L\times K$ and $M\times K$ so-called Vandermonde matrices, and C is a (full rank) diagonal amplitude matrix whose elements are given by $(C)_{kk} = c_k'' \equiv c_k \exp(i\varphi_0)$. (A double prime is used rather than a single one, the latter being reserved to denote a second dimension in 2-D modelling.) The symbol ~ denotes transposition. Eq.(4) can easily be checked by writing out the matrix multiplications. We call the decomposition of Eq.(4) the Vandermonde decomposition of the model function matrix. It is important to note that each row of a Vandermonde matrix is equal to the product of the previous row and the diagonal matrix $Z \stackrel{\text{def}}{=} \text{diag}(z_1, z_2, \ldots, z_K)$. This special structure arises through the property of exponentially damped sinusoids given in Eq.(3). The ***essence of the State Space method*** is that it brings about a Vandermonde decomposition of the data matrix X as closely as possible, i.e. in the least squares sense. After this has been achieved the wanted parameters are immediately available. For later use we call the quantities $z_k = \exp[(\alpha_k + i\omega_k)\Delta t]$, $k = 1, 2, \ldots, K$, the *signal poles*.

The Vandermonde decomposition of X is arrived at by first subjecting this matrix to Singular Value Decomposition (SVD, see e.g. ref. *20* for a tutorial), according to

$$X \;(L\times M) \;=\; U \;(L\times L) \;\; \Lambda \;(L\times M) \;\; V^{\dagger} \;(M\times M) \quad , \tag{5}$$

where U and V are unitary matrices of sizes $L\times L$ and $M\times M$, and whose columns are called *left* and *right singular vectors* respectively (in this example, $L \approx M/2$). The symbol † denotes hermitian conjugation. Λ is an $L\times M$ diagonal matrix whose diagonal entries are called *singular values*. The phases of the singular vectors are chosen such that the singular values are nonnegative. If the data are noiseless and comprise K exponentially damped sinusoids, then only K singular values are nonzero, i.e. one per sinusoid. The singular values are arranged according to descending magnitude. No loss of information is incurred if those parts of U, Λ, and V that are associated with the zero singular values are truncated. Thus if we retain only the shaded parts in the following equation, the result remains unchanged.

$$X \;(L\times M) \;=\; U_K \;(L\times K) \;\; \Lambda_K \;(K\times K) \;\; V_K^{\dagger} \;(K\times M) \tag{6}$$

We point out that each *non*exponentially decaying sinusoid gives rise to a *series* of nonzero singular values, rather than to a single one. In our experience such a series quickly tends to zero (ref. *22*). Apart from this, instrumental noise superimposed on the signal causes *all* singular values to be nonzero. The relative size of the noise-related singular values depends of course on the SNR. Usually, the distribution of singular values reveals which are related to the signal and which to the noise. Once the distinction between the two groups has been established (i.e., optimal value of K determined), the noise-related singular values are put to zero and truncation takes place as indicated before in Eq.(6).

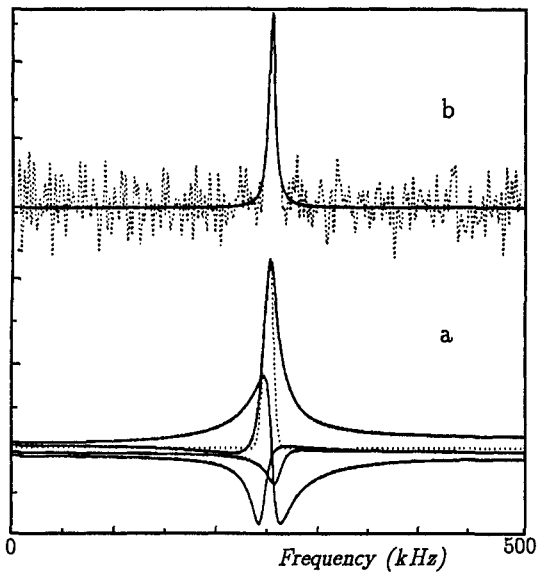

Fig.1 FFT of SVD-based quantification of a *non*exponentially damped sinusoid, $\exp(\beta t^2 + i\omega t)$. See (ref.*21*).
a) Noiseless case. The dotted line is the FFT of the signal. The drawn lines are the FFT's of the constituents of the decomposition into exponentially damped sinusoids.
b) Noise added. The dotted line is the FFT of the noisy signal. The drawn line is the FFT of the fitted model function. At the given SNR only one exponentially sinusoid was required.

Next, we state without proof (see ref. *13*) that it is always possible to transform the Vandermonde decomposition of Eq.(3) into a product of matrices that have the same structure and size as U_K, Λ_K, and V_K of the truncated singular value decomposition of the data matrix X, i.e.

$$\hat{X} = \zeta_{LK}\, C\, \tilde{\zeta}_{MK} = \hat{U}_K\, \hat{\Lambda}_K\, \hat{V}_K^{\dagger} \quad , \tag{7}$$

where the caret on $\hat{U}_K$, $\hat{\Lambda}_K$, and $\hat{V}_K^{\dagger}$ denotes that these matrices are related to the model function matrix rather than to the data matrix. It can be shown (ref. *13*) that the particular structure of the Vandermonde matrices ζ_{LK} and ζ_{MK} noted above is still present in $\hat{U}_K$ and $\hat{V}_K$, albeit in a somewhat more complicated form: each row of $\hat{U}_K$ (or $\hat{V}_K$) is equal to the product of previous row times a nonsingular $K \times K$ matrix denoted by $\hat{Z}$. The eigenvalues of $\hat{Z}$ are equal to the signal poles defined above. This important property points the way to modelling a measured signal with exponentially damped sinusoids. All one has to do (ref. *13*) is find a matrix Z' that relates successive rows of U_K, according to

$$\left((U)_{l+1,1}\ (U)_{l+1,2}\ \cdots\ (U)_{l+1,K}\right) = \left((U)_{l,1}\ (U)_{l,2}\ \cdots\ (U)_{l,K}\right) Z' \quad , l = 1,2,\ldots,L-1 \ , \tag{8}$$

and then compute its eigenvalues. If the signal is noiseless and exponentially damped, then the solution of Eq.(8) is exact. However, if noise is present and/or the damping is nonexponential, Eq.(8) is to be solved in the least squares sense, which is easily accomplished (ref. *13*). The special structure of Eq.(8) guarantees adherence to the exponentially damped model function of Eq.(1). Once Z' has been computed, the damping factors and frequencies follow from the eigenvalues of Z'. Subsequently, the amplitudes and phases can be found by fitting Eq.(1) to the data with the α_k and ω_k fixed to the values just obtained. For the sake of completeness, we mention that if the data matrix X is made square and all its rows (and columns) are linearly *in*dependent, then an exact Vandermonde decomposition exists (ref. *24*). In practice, the required linear independence is brought about by noise. Additional details on this modelling aspect are treated in (refs. *23,25,26*).

In summary, we have now discussed quantification of real-world 1-D time domain signals in terms of Eq.(1) with the aid of State Space modelling. The damping of the signals need not be exponential.

Rapid SVD of Hankel matrix

The computational load of SVD of a *general* matrix is proportional to the third power of the size of that matrix. Thus when the matrix at hand is large the State Space processing time may become prohibitively long. This problem has been addressed in e.g. (refs. *17,27-30*). One approach is to compute only the signal-related singular values and singular vectors (i.e., the shaded regions in Eq.(6)). Such a strategy can be successfully carried through by invoking the so-called Lanczos algorithm (*17*). Treatment of this algorithm is beyond the scope of this paper. For details the reader is referred to (refs. *17,31,32*). Here we restrict ourselves to the aspect of exploiting the symmetry of a Hankel matrix in the quest for further reduction of the computational load. Following a suggestion by P.C. Hansen (*33*), it was recently established (*23,25*) that the Lanczos algorithm is well suited for this purpose too. To explain this feat we mention that the Lanczos algorithm is iterative, the most time-consuming part of each iteration consisting of two matrix-vector multiplications, namely Xv_a and $\tilde{X}v_b$, where X is the data matrix and v_a and v_b are vectors, and the symbol $\sim$ indicates transposition. It follows then that reduction of the computing time of Xv_a and $\tilde{X}v_b$ would yield the desired acceleration. We shall see below for Xv_a that the Hankel symmetry of X enables one to accomplish this. A similar procedure applies to $\tilde{X}v_b$.

First, should $N \neq 2^I$, where I is an integer, we zero-fill both the data and the vector v_a to the nearest power of two. Then we note that X can be embedded in a so-called circulant matrix (ref. *34*) defined in Figure 2. As can be seen each row of a (left) circulant matrix is related to the next one by cyclic permutation (to the left). The data matrix X resides in the upper left rectangle of the circulant matrix.

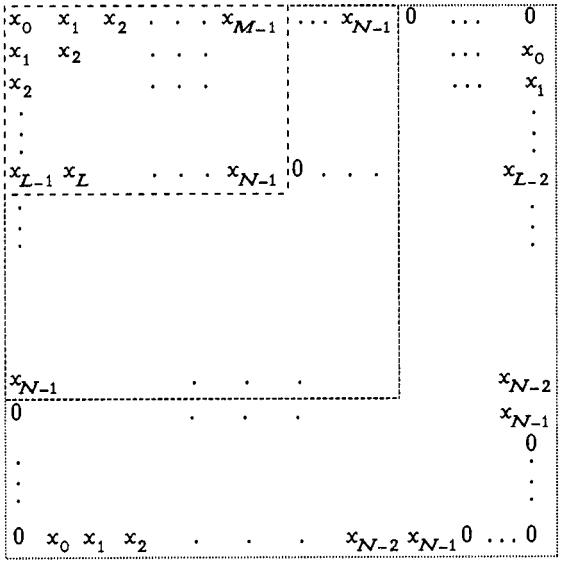

Figure 2. Formation of a circulant matrix Y from the data x_n, $n = 0, \ldots, N-1$, (zero-filled to the nearest power of two if $N \neq 2^I$). Each row is related to the next one by a cyclic permutation. The data matrix X is a subunit of Y, residing in the upper left rectangle. Any multiplication Xv_a can be replaced by Yv_a', where v_a' is the zero-filled version of v_a. If N is large Yv_a' can be executed swiftly by invoking FFT, using Eq.(9).

A very useful property of circulant matrices is that they can be decomposed as (ref. *34*)

$$Y = \Gamma F^{-1} D F \quad , \tag{9}$$

in which Γ is in turn a left circulant matrix whose first row equals $(1,0,0,\ldots,0)$, F is the well-known FFT matrix of size 2^I, and D is a diagonal matrix whose diagonal entries are equal to the eigenvalues of ΓY. The latter eigenvalues can be obtained at little cost using the special properties of circulant matrices (*34*); moreover, they need only be calculated in the first iteration. Using Eq.(9), it can be seen that the product of Y and a vector can be executed swiftly by applying FFT and its inverse, plus some additional operations involving Γ and D. Finally, it can be seen that the product Xv_a can be replaced by Yv_a', where v_a' is the zero-filled version of v_a, and retaining only the first L entries of the result. In this way the most time-consuming part of each Lanczos iteration can be accelerated for the case of large N. Note that only one row of the large circulant matrix Y need be stored in memory.

It follows from the above that spectacular reductions of the SVD computation time can be achieved when N is large and the required number of singular values and vectors is relatively small. In other situations, the gain is smaller. One aspect to be reckoned with is that the number of required iterations becomes large when adjacent singular values get close to each other. In actual practice, the latter occurs when the smallest signal-related singular values are barely distinguishable from noise-related singular values. In this situation a suitable compromise between good modelling (more singular values) and computation time (fewer singular values) is to be found. Using real-world magnetic resonance measurements with N=1024 we found reductions of the computation ranging from several hundred to two (refs. *23,35*) The latter reductions are relative to the so-called normal equations approach to SVD, as applied in (ref. *36*).

2–D signals

Usually, 2-D signals $x_{nn'}$, $n=0,1,\ldots,N-1$, $n'=0,1,\ldots,N'-1$, are processed in 1-D fashion. Forming an $N\times N'$ matrix from the data, this amounts to processing the data first row by row and subsequently column by column, similar to the procedure followed with 2-D FFT. A consequence of this approach is that the number of data points involved per fit is relatively small, namely N or N'. In addition, one has to fit frequencies and damping factors again and again for each consecutive row or column while such parameters are known to be constant. Fitting a 2-D model function to all $N\times N'$ data points concurrently lacks the two unfavourable properties just mentioned, and is therefore to be preferred. In the following we propose a 2-D State Space method that is capable of using all data points concurrently. In addition we point at some pitfalls attendant to the 2-D case and indicate how the proposed method circumvents such complications.

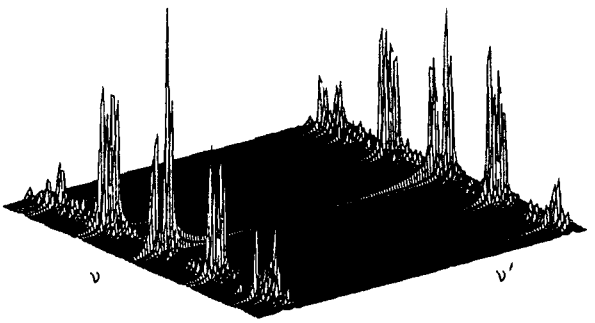

Fig. 3. Magnitude FFT of a 2-D NMR COSY signal comprising 256×128 data points. The unprimed dimension comprises many more spectral components than the primed dimension. See Fig. 4 for singular values in each dimension.

The model function used is a sum of products of 2-D exponentially damped sinusoids, i.e.

$$\hat{x}_{nn'} = \sum_{k=1}^{K}\sum_{k'=1}^{K'} c_{kk'}\exp(i\varphi_{kk'})\exp[(\alpha_k+i\omega_k)t_n+(\alpha'_{k'}+i\omega'_{k'})t'_{n'}] \quad , \tag{10}$$

where we distinguish a primed and an unprimed dimension, the meaning of the symbols being the same as in Eq.(1). Note that K need not be equal to K' and the $K\times K'$ amplitudes may all be nonzero. It can easily be checked by writing out that the matrix $\hat{X}$ formed from the $N\times N'$ data points can be decomposed into a product of two Vandermonde matrices and an amplitude, similar to Eq.(4)

$$\hat{X} = \begin{pmatrix} 1 & \cdots & 1 \\ z_1^1 & \cdots & z_K^1 \\ \vdots & & \vdots \\ z_1^{N-1} & \cdots & z_K^{N-1} \end{pmatrix} \begin{pmatrix} c''_{11} & \cdots & c''_{1K'} \\ \vdots & & \vdots \\ c''_{K1} & \cdots & c''_{KK'} \end{pmatrix} \begin{pmatrix} 1 & z_1'^1 & \cdots & z_1'^{N'-1} \\ \vdots & \vdots & & \vdots \\ 1 & z_{K'}'^1 & \cdots & z_{K'}'^{N'-1} \end{pmatrix} \quad , \tag{11}$$

$$= \qquad \zeta_{NK} \qquad\qquad C'' \qquad\qquad \tilde{\zeta}'_{N'K'}$$

where the double prime on $c''_{kk'}$ and C'' indicates that the phase has been incorporated in these quantities as before.

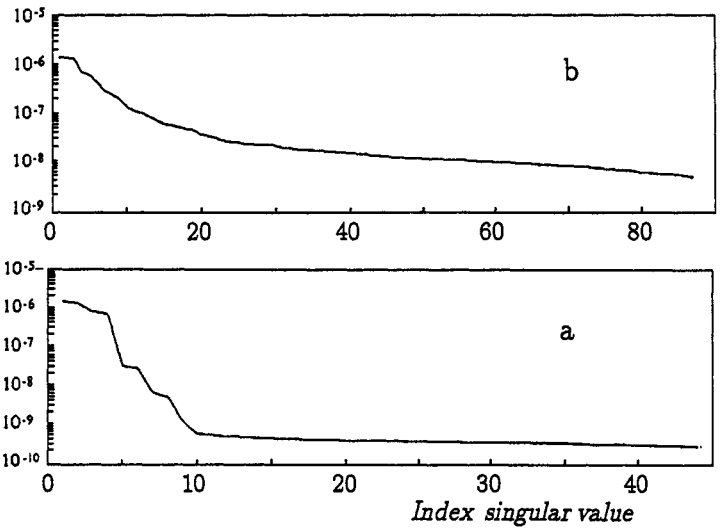

Fig.4 Singular value plots (log. scale) of the 2-D real-world NMR time domain signal whose spectrum is shown in Fig. 3. a) Singular values for the (primed) dimension comprising fewest spectral components. A clear transition from signal-related singular values to noise-related singular values can be discerned at index≈10. b) Singular values for the 'crowded' (unprimed) dimension. Here it is difficult to establish the number of signal-related singular values. This result indicates that proper quantification is problematic with whatever method.

In general, C'' is not square and diagonal, contrary to the 1-D case. See e.g. Fig. 3. However, if C'' happens to be square and all its rows and columns are linearly independent, then the Vandermonde decomposition and the (noise-truncated) SVD yield matrices of the same size so that the fit can proceed in almost the same way as above. The only difference is that now both the left and the right singular vectors are involved, yielding respectively the unprimed and primed damping factors and frequencies. The amplitudes and phases are obtained by linear least squares fitting of Eq.(10) to the data with the damping factors and frequencies fixed to the previously obtained values.
Next, we consider the case that the rank of C'' equals one, i.e. all rows (columns) of C'' are multiples of each other. It can be shown (ref. *25*) that in absence of noise, SVD of the data matrix then yields only one nonzero singular value, irrespective of the number of spectral components in either dimension. Under this condition the constituents of the Vandermonde decomposition and the SVD have different sizes so that the usual procedure ceases to work. Although this example constitutes a highly improbable worst case, it indicates that the method must be adapted in such a manner that the number of nonzero singular values always reflects the number of spectral components. At the same time the aim that all data be involved concurrently should be satisfied.

A solution to the rank-related problem just noted has recently been given in (refs. *25,37*). First one constructs a Hankel data matrix H_n from each row $x_{nn'}$, $n' = 0,1,\ldots,N'-1$, and n fixed, of the 2-D data matrix. Then one concatenates these Hankel matrices H_n, $n = 0,1,\ldots,N-1$, into a large block Hankel matrix $H = (H_0\ H_1\ \ldots\ H_{N-1})$. Note that all data points are contained in H. It can be shown that the number of singular values of H always corresponds to the number of spectral components K' present in the primed dimension, so long as the number of rows and columns of H_n equals at least K'. This in turn implies that the primed damping factors and frequencies can always be obtained from the left singular vectors of H. The computation time of the SVD of the large matrix H can be limited by invoking the normal equations approach which amounts to diagonalizing the relatively small matrix $HH^\dagger = \sum_{n=0}^{N-1} H_n H_n^\dagger$. The computing time required to carry out the product $HH^\dagger$ can in turn also be limited because of the block Hankel structure of H. Subsequently, transposition of the 2-D data matrix and repetition of the procedure yields the unprimed damping factors and frequencies. Finally, the amplitudes and phases follow from the same linear least squares procedure encountered above.

An application of the 2-D method to a simulated signal with $K=3$ and $K'=4$ has been treated in (ref. *37*). In this example several of the 3×4 amplitudes were made smaller than the standard deviation of the added noise. Fifty quantification trials were run using different realizations of the noise. Each time the quantification was successful, the standard deviation of the resulting parameters being less than twice the Cramér-Rao lower bound.

An application to a real-world 2-D NMR COSY measurement has been treated in (ref. *38*). The magnitude FFT of the data is shown in Fig. 3. It can be seen that the number of spectral components in the unprimed dimension is much higher than that in the primed dimension. This fact is reflected in the plots of the singular values for both dimensions, given in Fig. 4. From the abrupt end of the 'noise plateau' (looking from right to left) in Fig. 4a one can infer that only about ten exponentially damped sinusoids are required to model the signal in the primed dimension. On the other hand, perusal of Fig. 4b suggests that many tens of sinusoids are required to model the signal in the unprimed dimension. The latter result indicates that either the number of spectral components is very high and/or that the damping deviates substantially from exponential. Consequently, at the very least the singular value plot serves here as a warning that estimation of the unprimed parameters is difficult to achieve with whatever method. With the method presented here quantification was feasible using $K=70$ and $K'=10$, which among other things involved estimation of 700 complex-valued amplitudes. Further details are given in (refs. *38*,*39*). See e.g. (ref. *40*) for an introduction to the COSY technique, and (ref. *41*) for an alternative approach to 2-D time domain signal processing.

An aspect requiring further research is that distinction between sinusoids that have the same frequency but different damping factors is difficult. As a result, all sinusoids whose frequencies coincide (see Fig. 3) usually end up with one and the same damping factor, unless the SNR is very high. Should this lead to unacceptable errors, then one has to resort to an additional round of nonlinear least squares fitting of the damping factors, using fixed values of the frequencies yielded already by the 2-D State Space method (ref. *39*). The damping factors yielded by the 2-D State Space method can serve as starting values.

CONCLUSIONS

We have shown that quantification of Magnetic Resonance time domain signals can be effected without much user involvement by invoking State Space modelling. A simple mathematical description of State Space modelling in terms of Vandermonde decomposition and Singular Value decomposition (SVD) was presented. Although State Space modelling uses exponentially damped sinusoids as basis functions, it appeared also capable of quantifying signals that are damped nonexponentially. The computation time of SVD was also addressed. It was shown how the Hankel symmetry of the data matrix attendant to a 1-D signal can be exploited to achieve a significant reduction of the computation time. Finally, a form of 2-D State Space modelling using all 2-D data concurrently was treated.

Acknowledgements

This work was supported by the FOM/STW Research Foundations. The authors thank A. van den Boogaart, R. van Duuren, A.F. Mehlkopf, and J. Zonneveld for cooperation and useful discussions.

REFERENCES

1. J.C. Haselgrove, H. Subramanian, R. Christen, J.S. Leigh, Rev. Magn. Reson. Med., **2**, 167 (1987).
2. D.S. Stephenson, Prog. NMR Spectrosc., **20**, 515 (1988).
3. R. de Beer, D. van Ormondt, W.W.F. Pijnappel, Israel J. Chem., **28**, 249 (1988).
4. J.C. Hoch, Methods in Ezymology, **176**, 216 (1989).
5. H. Gesmar, J.J. Led, F. Abildgaard, Prog. NMR Spectrosc., **22**, 255 (1990).
6. R. Roy, B.G. Sumpter, G.A. Pfeffer, S.K. Gray, D.W. Noid, Phys. Rep., **205**, 109 (1991).
7. A. Tarantola, *Inverse Problem Theory*, Elsevier, Amsterdam (1987).
8. R. Gonin and A.H. Money, *Nonlinear L_p-Norm Estimation*, Dekker, New York (1989).
9. K. Sekihara and N. Ohyama, Magn. Reson. Med., **13**, 332 (1990).
10. P. Wayner, Byte, **16**, no.1, 361 (Jan. 1991).

11. G.L. Bretthorst, J. Magn. Reson., **93**, 369 (1991).
12. R. Kumaresan and D.W. Tufts, IEEE Trans. ASSP-**30**, 833(1982).
13. S.Y. Kung, K.S. Arun, D.V.B. Rao, J. Opt. Soc. Am., **73**, 1799 (1983).
14. M. Aoki, *State Space Modeling of Time Series*, 2nd Ed.,Springer, Berlin (1990).
15. H. Barkhuysen, R. de Beer, and D. van Ormondt, J. Magn. Reson., **73**, 553 (1987).
16. H. Yan and J.C. Gore, J. Magn. Reson., **80**, 324 (1988).
17. G.L. Millhauser, A.A. Carter, D.J. Schneider, J.H. Freed, R.E. Oswald, J. Magn. Reson., **82**, 150 (1989).
18. S. Mayrargue and J.P. Jouveau, in: *Signal Processing IV. Theories and Applications*, J.L. Lacoume, A. Chehikian, N. Martin, and J. Malbos Eds., North Holland, Amsterdam, pp. 55-58 (1988).
19. A.C. Kot, S. Parthasarathy, D.W. Tufts, and R.J. Vaccaro, Proc. Int. Conf. Acoust., Speech, Signal Processing, IEEE, pp. 1549-1552 (1987).
20. G. Strang, *Linear Algebra and its Applications*, Hartcourt Brace Jovanovitch, San Diego (1988).
21. H. Barkhuysen, R. de Beer, A.C. Drogendijk, D. van Ormondt, and J.W.C. van der Veen, in: Proc. International School of Physics "Enrico Fermi" on the *Physics of NMR Spectroscopy in Biology and Medicine*, B. Maraviglia Ed., Italian Physical Society, pp. 313-344 (1988).
22. R. de Beer and D. van Ormondt, in: *In vivo Magnetic Resonance Spectroscopy*, M.Rudin and J. Seelig Eds., Springer, in press (1991).
23. W.W.F. Pijnappel, R. de Beer, and D. van Ormondt, J. Magn. Reson., in press (Feb. 1992).
24. M. Fiedler, *Special Matrices and their Applications in Numerical Mathematics*, Martinus Nijhoff, Dordrecht (1986).
25. W.W.F. Pijnappel, *Quantification of 1-D and 2-D Magnetic Resonance Spectroscopic Data*, PhD Thesis, Delft University of Technology (February 1991).
26. I. Dologlou and G. Carayannis, Signal Processing, **23**, 293 (1991).
27. J. Tang, C.P. Lin, M.K. Bowman, and J.R. Norris, J. Magn. Reson., **62**, 167 (1985).
28. H. Barkhuysen, R. de Beer, and D. van Ormondt, J. Magn. Reson., **64**, 343 (1985).
29. P. Comon, in: *Signal Processing IV. Theories and Applications*, J.L. Lacoume, A. Chehikian, N. Martin, and J. Malbos Eds., North Holland, Amsterdam, pp. 647-650 (1988).
30. S. van Huffel, J. Comput. Appl. Math., **33**, 105 (1990).
31 J.K. Cullum and R.A. Willoughby, *Lanczos Algorithms for Large Symmetric Eigenvalue Computations*, Vols. I and II, Birkhäuser, Boston (1985).
32. G.H. Golub and C.F. Van Loan, *Matrix Computations*, 2nd Ed., Johns Hopkins, Baltimore (1990).
33. P.C Hansen, Internal Report, Technical University of Denmark, Lyngby, Denmark (1988).
34. P.J. Davis, *Circulant Matrices*, Wiley, New York (1979).
35. A. van den Boogaart, M. Sc. Thesis (in Dutch), Delft University of Technology (June 1991).
36. H. Barkhuysen, R. de Beer, and D. van Ormondt, J. Magn. Reson., **64**, 343 (1985).
37. R. de Beer, D. van Ormondt, and W.W.F. Pijnappel, Proc. Int. Conf. Acoust., Speech, Signal Processing, IEEE, pp. 1504-1507 (1989).
38. R. van Duuren, M. Sc. Thesis (in Dutch), Delft University of Technology (June 1991).
39. J. Zonneveld, M. Sc. Thesis, Delft University of Technology (March 1991).
40. A. Schweiger, Angew. Chem. Int. Ed. Engl., **30**, 265 (1991).
41. J. Gorcester and J.H. Freed, J. Magn. Reson. **78**, 292 (1988). This work also mentions exploitation of the Hankel symmetry in Lanczos SVD, but does not elaborate on this aspect.